Inelastic Neutron Scattering Spectrum and Quantum Mechanical Calculations on the Internal Vibrations of Pyrimidine

ARTICLE *in* THE JOURNAL OF PHYSICAL CHEMISTRY A · JULY 1999

Impact Factor: 2.69 · DOI: 10.1021/jp991173h

4 AUTHORS, INCLUDING:

Manuel Fernandez-Gomez
Universidad de Jaén
93 PUBLICATIONS **675** CITATIONS
SEE PROFILE

J. J. López González
Universidad de Jaén
134 PUBLICATIONS **1,136** CITATIONS
SEE PROFILE

M. Paz Fernández-Liencres
Universidad de Jaén
27 PUBLICATIONS **234** CITATIONS
SEE PROFILE

Inelastic Neutron Scattering Spectrum and Quantum Mechanical Calculations on the Internal Vibrations of Pyrimidine

Amparo Navarro,* Manuel Fernández-Gómez, Juan J. López-González, and M. Paz Fernández-Liencres

Department of Physical and Analytical Chemistry, University of Jaén, 23071 Jaén, Spain

E. Martínez-Torres

Department of Physical Chemistry, University of Castilla-La Mancha, 13003 Ciudad Real, Spain

J. Tomkinson

Rutherford Appleton Laboratory, Chilton, OX11, United Kingdom

G. J. Kearley

Institut Laue Langevin, BP 156, 38042 Grenoble, Cedex 09, France

Received: April 7, 1999

A vibrational analysis of the inelastic neutron scattering spectrum (INS) of pyrimidine has been carried out combined with quantum mechanical calculations at the RHF, MP2, and B3LYP levels using the 6-31G* basis set in all the cases. The INS spectrum was first calculated from the atomic displacement matrix in order to determine which level of theory gives the best agreement between observed and calculated INS intensities. In a second approach, force constants from a calculation at the MP2/6-31G* level were transformed to a symmetrized set (C_{2v}) and all the diagonal and some off-diagonal force constants were fitted. Good agreement between observed and calculated wavenumbers and spectral INS intensities was achieved which demonstrates the validity of our force field.

I. Introduction

Pyrimidine is by far the most ubiquitous member of the diazines family, with uracil and tymine being constituents of RNA and DNA, respectively, and with cytosine being present in both. The pyrimidine skeleton is also present in many natural products, such as vitamin B_1 (thiamine), and many synthetic compounds, such as barbituric acid, and hypnotics, such as veronal.[1]

From a vibrational point of view, the pyrimidine molecule has been extensively studied both from theoretical and experimental approaches. This molecule has C_{2v} symmetry, with 24 normal modes distributed as: nine A_1 (IR, Raman) + eight B_1 (IR, Raman) + two A_2 (Raman) + five B_2 (IR, Raman). The infrared and Raman spectra in different phases and under different experimental conditions have been reported,[2−13] and a variety of force fields calculations have been performed at the empirical,[14,15] semiempirical,[16] Hartree−Fock,[17,18] and DFT[19] levels. The first vibrational assignments were made by Ito et al.[2] and Lord et al.[3] who set up a correlation with the benzene assignments. Simmons and Innes[5] proposed a new assignment for the A_1 fundamentals from the infrared and Raman spectra. Sbrana et al.[6] studied the infrared spectrum of pyrimidine at liquid nitrogen temperature and in nonpolar solvents. Milani-Nejad and Stidham[11] prepared several different deuterated pyrimidines of C_{2v} symmetry and recorded their IR and Raman spectra. Bokobza-Sebagh and Zarembowitch[12] investigated the infrared and Raman spectra of pyrimidine and its pentachloroiridium (III) complex. Finally, Unemoto et al.[13] re-examined the out-of-plane vibrational assignments and reassigned some fundamentals. The vibrational assignments from all these experimental works are collected in Table 1.

Two empirical force fields have been obtained for pyrimidine so far. The first normal coordinate analysis was made by Berezin and Potapov[14] using a set of primitive coordinates. Later, Anantharama Sarma[15] determined the in-plane Urey−Bradley and VFF-type force fields of pyrimidine. The first quantum mechanical force field was derived by Wiberg in 1990,[17] at RHF/6-31G* and RHF/6-31+G* levels. More recently, G. Pongor et al.[18] calculated an a priori scaled quantum mechanical (SQM) force field for pyrimidine, at the RHF/4-21G level of theory. Later, Magdó et al.[16] carried out a new scaled force field at the MINDO/3 level for different azines, including pyrimidine. Finally, in 1996, Martin and Van Alsenoy[19] performed a DFT study for different azines including pyrimidine by using the B3LYP exchange-correlation functional with cc-pVD(T)Z basis sets. In all these analyses, the agreement between observed and calculated frequencies was good, except for the out-of-plane normal modes whose assignments are less certain.

Thus, while new pyrimidine derivatives have been studied by various spectroscopies,[20,21] the assignments given for the parent molecule, especially for the out-of-plane vibrations, remain subject to question. In this sense, the inelastic neutron scattering (INS) technique is well adapted to study the low-energy region and offers several advantages over optical

* E-mail: anavarro@ujaen.es.

10.1021/jp991173h CCC: $18.00
Published on Web 07/03/1999

TABLE 1: Vibrational Assignments for the Pyrimidine Molecule (cm^{-1})

		IR, Raman[a]	IR[b]	IR[c]	sol	IR[d]	cryst.	IR, Raman[e]	IR[f]	Raman[f]	Raman[g]
	ν_{20a}	3083	3090	3078	3084			3074	3082	3084	
	ν_2	3048	3055	3050	3046			3052	3047	3050	
	ν_{13}	3001		3002	3003			3038	3002	3000	
	ν_{8a}	1570	1572	1570	1577			1564	1565	1567	
A_1	ν_{9a}	1467	1465	1402	1398		1398	1397.5	1396	1399	
	ν_{9a}	1141	1148	1138	1135		1143	1139	1136	1139	
	ν_{12}	1066	1066	1068	1066		1086	1065	1066		
	ν_1	991	992	993	987		992	991.5	990	991	
	ν_{6a}	624	678	677	676		673	678	678	679	
	ν_{7b}	3095		3095				3086	3039	3039	
	ν_{8b}	1570		1559	1568			1568	1569	1570	
	ν_{19b}	1402		1466	1462		1473	1466	1465	1466	
	ν_{14}	1371		1355	1373		1380	1370	1355	1359	
B_1	ν_3	1227		1223	1221		1233	1225	1224	1229	
	ν_{15}	1161		1154	1156		1162	1159	1156		
	ν_{18b}	1021		1075	1020		1024	1071	1067		
	ν_{6b}	567		621	620		628	623	622	623	
A_2	ν_{17a}	870		870							1004
	ν_{16a}	394		394	394			398.5			395
	ν_4	679		709	704		717	708	720		775
	ν_5	980		993	975		980	980	980	980	
B_2	ν_{10b}	722		719	801		831	721		955	982
	ν_{11}	806		804	710		720	811	810		725
	ν_{16b}	344		344	343		342	344	346	349	345

[a] From ref 3. [b] From ref 5. [c] From ref 6. [d] From refs 7 and 9. [e] From ref 11. [f] From ref 12. [g] From ref 13.

spectroscopies. First, there are not selection rules,[22−25] but because of the large incoherent cross section of hydrogen atoms, INS spectra are dominated by vibrations involving hydrogen motions,[23] which is sometimes referred to as the "*hydrogen selection rule*". Second, the most important advantage is that INS intensities are relatively simple to calculate from the vibrational amplitudes so that they can supplement the wavenumber data in the force field analysis. Ab initio, semiempirical, or force field Wilson GF methods[26] can be used to generate the vibrational frequency and amplitude data from which the INS spectrum can be simulated. In this way, the results of calculations can be tested against experiment in a straightforward way. We go one stage further by using the CLIMAX program[27] to read the force constants matrix in Cartesian coordinates from GAUSSIAN, transform these up to internal or symmetry coordinates, and then refine the force constants so as to minimize the difference between observed and calculated INS spectra.

Thus, CLIMAX can be used to test what level of theory chosen in our particular calculation is the best in order to reproduce the INS intensity. This procedure has been already carried out for *sym*-triazine, trichloro-*sym*-triazine, and pyrazine,[28,29] which provided excellent agreement between observed and calculated spectra. However, the ability to obtain good agreement is limited by the strength of intermolecular interactions. CLIMAX, and most semiempirical and ab initio methods, use by default the isolated molecule approximation, while INS spectroscopy only provides good quality spectra for the crystalline state at liquid helium temperatures.

In this work, we present a general review of the vibrational spectrum of pyrimidine as a basis for our analysis of the INS spectrum in order to clarify the assignment of the fundamental modes.

II. Experimental Section

Pyrimidine was obtained from Aldrich and purified by repeated distillation under reduced pressure. About 1 g of sample was wrapped in aluminum foil under a dry atmosphere and loaded into a standard liquid helium cryostat controlled at 5 K. The INS spectrum was obtained on the time-focused crystal analyzer spectrometer TFXA at ISIS pulsed neutron source of the Rutherford Appleton Laboratory, UK, which has an energy resolution $\Delta h\omega/h\omega \leq 2\%$. The total counting time was 24 h. Conversion of the raw INS spectrum from time-of-flight to $S(Q,\omega)$ and correction for background scattering was achieved using standard procedures.

The gas-phase IR spectrum was measured on a Vector 22 Bruker FT-IR spectrometer using a Specac heated 10 cm path cell with KBr windows and working at room temperature.

III. Computational Details

III.1. Quantum Mechanical Calculations. We have performed ab initio calculations using GAUSSIAN/94[30] at different levels of theory, i.e., RHF,[31] MP2,[32] and DFT-B3LYP,[33] with the 6-31G* basis set for the pyrimidine molecule in order to test the potential energy minimum at each level. The force constant matrix in Cartesian coordinates from GAUSSIAN was transformed into both an internal and symmetry coordinates bases using CLIMAX. An independent symmetry coordinate set was constructed by diagonalizing the $\mathbf{BB}^t$ matrix ($\mathbf{B} = UB$). The eigenvectors associated with zero eigenvalues correspond to the null coordinates, and then the independent symmetry coordinates were obtained by orthogonalization using the Schmidt procedure.[34] The symmetry coordinates are listed in Table 2, although it is worth noting that the choice is not unique. The definition of internal coordinates was made according to Figure 1.

III.2. Calculation of INS Spectrum. CLIMAX produces $S(Q,\omega)$ intensities taking full account of the Debye−Waller factor for the fundamentals, overtones, combinations, and external thermal vibrations.[24] By default, the frequencies and atomic displacements are calculated from the force constant matrix using the GF Wilson method, and the INS intensities are calculated according to the theory given by Tomkinson et al.[35,36] External thermal vibrations shift part of the internal mode spectral intensity into "phonon wings". These wings mimic the external density of states spectrum of the sample and attenuate

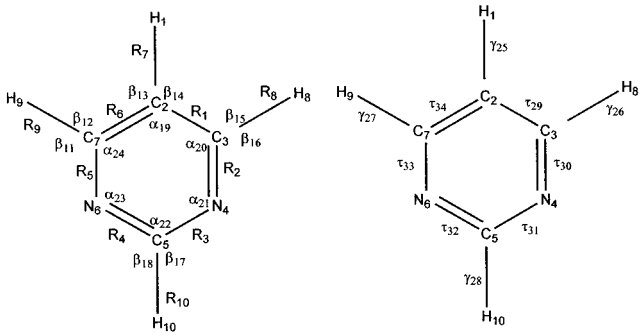

Figure 1. Atom numbering and internal coordinates defined in pyrimidine.

TABLE 2: Symmetry Coordinates for Pyrimidine

		symmetry coordinates
A_1	S_1	$0.09668(R_1 + R_2) + 0.69307(R_2 + R_5) + 0.1015575(R_3 + R_4)$
	S_2	$0.65409\alpha_{19} - 0.50455(\alpha_{20} + \alpha_{24}) + 0.17751(\alpha_{21} + \alpha_{23})$
	S_3	$0.22700\alpha_{19} - 0.01488(\alpha_{20} + \alpha_{24}) - 0.46052(\alpha_{21} + \alpha_{23}) + 0.7240\alpha_{22}$
	S_4	$-0.35816\alpha_{19} - 0.16870(\alpha_{20} + \alpha_{24}) + 0.18034(\alpha_{21} + \alpha_{23}) + 0.33488\alpha_{22} + 0.40895(R_1 + R_6) - 0.38931(R_3 + R_4)$
	S_5	$0.01461\alpha_{19} + 0.00688(\alpha_{20} + \alpha_{24}) - 0.00735(\alpha_{21} + \alpha_{23}) - 0.01366\alpha_{22} + 0.48712(R_1 + R_6) - 0.14015(R_2 + R_5) + 0.49272(R_3 + R_4)$
	S_6	R_7
	S_7	$R_8 + R_9$
	S_8	R_{10}
	S_9	$(\beta_{11} - \beta_{12}) - (\beta_{15} - \beta_{16})$
B_1	S_{10}	$R_8 - R_9$
	S_{11}	$\beta_{17} - \beta_{18}$
	S_{12}	$\beta_{13} - \beta_{14}$
	S_{13}	$(\beta_{11} - \beta_{16}) - (\beta_{12} - \beta_{15})$
	S_{14}	$-0.45680(R_1 - R_6) + 0.53976(R_3 - R_4)$
	S_{15}	$0.44511(R_1 - R_6) - 0.39997(R_2 - R_5) + 0.37670(R_3 - R_4)$
	S_{16}	$-0.50351(\alpha_{20} - \alpha_{24}) + 0.49647(\alpha_{21} - \alpha_{23})$
	S_{17}	$0.24808(R_1 - R_6) + 0.47380(R_2 - R_5) + 0.20995(R_3 - R_4) - 0.28939(\alpha_{20} - \alpha_{24}) - 0.29349(\alpha_{21} - \alpha_{23})$
A_2	S_{18}	$0.30494(\tau_{29} + \tau_{34}) - 0.57235(\tau_{30} + \tau_{33}) + 0.28182(\tau_{31} + \tau_{32})$
	S_{19}	$0.65694(\gamma_{26} - \gamma_{27}) - 0.18541(\tau_{29} + \tau_{34}) - 0.00803(\tau_{30} + \tau_{33}) + 0.18435(\tau_{31} + \tau_{32})$
B_2	S_{20}	$-0.45679(\tau_{29} - \tau_{34}) + 0.53976(\tau_{31} - \tau_{32})$
	S_{21}	$0.44511(\tau_{29} - \tau_{34}) - 0.39997(\tau_{30} - \tau_{33}) + 0.37670(\tau_{31} - \tau_{32})$
	S_{22}	$0.62674\gamma_{25} + 0.77923\gamma_{28}$
	S_{23}	$-0.31974\gamma_{25} + 0.64484(\gamma_{26} + \gamma_{27}) + 0.25717\gamma_{28}$
	S_{24}	$0.63450\gamma_{25} + 0.25907(\gamma_{26} + \gamma_{27}) - 0.51033\gamma_{28} + 0.13747(\tau_{29} - \tau_{34}) + 0.26256(\tau_{30} - \tau_{33}) + 0.11634(\tau_{31} - \tau_{32})$

the internal mode intensity by a Debye−Waller factor of $\exp(-Q^2U^2)$, where Q is the momentum transfer, which depends only on the spectrometer, and U^2 is the total mean-square amplitude of the scattering atom in the lattice vibrations.

IV. Results and Discussion

IV.1. Geometry Optimization. The geometry optimization of pyrimidine leads to a planar conformation (C_{2v}) at all levels of theory (RHF, MP2, and DFT). Table 3 contains the calculated geometrical parameters (bonds lengths and valence angles) obtained in the different calculations (without empirical corrections) along with electron diffraction parameters.[37] For the CH bond distances, RHF gives a deviation of 0.02 Å and MP2 and B3LYP of 0.01 Å; a better agreement was obtained by Martin and Van Alsenoy,[19] where the CH bond distances were calculated with a deviation of about 0.002 Å. For the CC and CN bond distances, the best agreement is obtained for MP2 and B3LYP, with deviations between 0.002 and 0.0004 Å. In general, the standard deviations, σ_{n-1}, in the bond distances are 2.049×10^{-2}, 7.801×10^{-3}, and 7.813×10^{-3} Å, for RHF, MP2, and B3LYP, respectively, which are acceptable. In relation to the bond angles, the standard deviations are 0.75°, 0.41°, and 0.50° for RHF, MP2, and B3LYP, respectively.

TABLE 3: Comparison of Experimental and Calculated Structural Parameters for Pyrimidine (in Å and deg)

	RHF/6-31G* [a]	MP2/6-31G* [a]	B3LYP/6-31G* [a]	exptl[b]
C_2C_3	1.382	1.393	1.394	1.393(2)
C_3N_4	1.321	1.344	1.339	1.340(2)
N_4C_5	1.317	1.343	1.338	1.340(2)
H_1C_2	1.073	1.085	1.085	1.099(7)
H_8C_3	1.076	1.088	1.089	1.099(7)
$H_{10}C_5$	1.075	1.088	1.089	1.099(7)
$H_1C_2C_3$	122.01	121.55	121.78	121.60
$H_8C_3N_4$	116.53	116.27	116.40	115.3(3)
$N_6C_5H_{10}$	116.56	116.30	116.30	116.20
$C_3C_2C_7$	115.99	116.89	116.43	116.80
$C_2C_3N_4$	122.33	122.27	122.42	122.30
$C_3N_4C_5$	116.23	115.58	115.67	116.80
$N_4C_5N_6$	126.88	127.40	127.40	127.6(3)

[a] This work. [b] From ref 37.

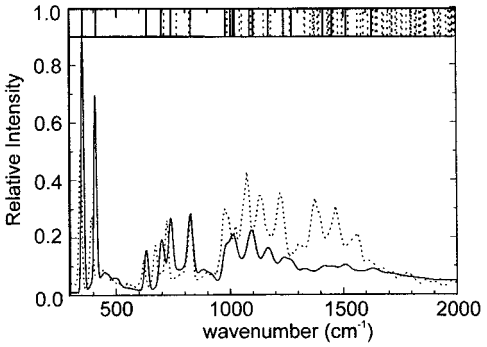

Figure 2. Observed (dot line) and calculated (continuous line) INS spectra of pyrimidine from the vibrational frequencies and atomic displacements using the MP2/6-31G* level. Solid bars at the top of the figure show frequencies of fundamentals, and broken lines show overtones and combinations.

IV.2. Spectral ab Initio Calculation. Due to the harmonic approximation used in our calculations, the largest differences between observed and calculated frequencies were obtained for the CH stretching normal modes, where the standard deviations were 377, 206, and 150 cm^{-1} for RHF, MP2, and B3LYP, respectively. For the remaining in-plane normal modes, the standard deviation were 153, 71, and 52 cm^{-1} for RHF, MP2, and B3LYP, respectively. For the out-of-plane normal modes, the standard deviations were 95, 42, and 24 cm^{-1} for RHF, MP2, and B3LYP, respectively. The wavenumbers from the different levels of calculation are collected in Table 4, and it can be seen that an important improvement is obtained for geometry and frequencies when electron correlation is introduced in the definition of the Hamiltonian, as expected.

We have also calculated the INS spectrum directly from ab initio and DFT calculations, and all levels of theory give similar results from the INS intensity point of view. Figure 2 shows the calculated INS spectra from the B3LYP/6-31G* level together with the observed spectrum, from which it can be seen that while the positions of the normal modes are close to those observed, there are some serious differences in intensities. This difference could be corrected by a refinement of the corresponding force constant matrix.

IV.3. Spectral Fitting and Force Field Refinement. We have carried out a refinement calculation of the force field for the pyrimidine molecule in symmetry coordinates for both in-

TABLE 4: Calculated, Observed, and Refined Values for the Vibration Frequencies (cm^{-1}) of the Pyrimidine Molecule

		RHF/6-31G*	MP2/6-31G*	B3LYP/6-31G*	INS	refined	PED (>10%)	assignments
A_1	ν_{20a}	3410	3265	3222	3074	3074	$97S_7$	CH str
	ν_2	3396	3241	3190	3052	3052	$43S_6 + 54\ S_8$	CH str
	ν_{13}	3371	3225	3174	3038	3038	$54S_6 + 44S_7$	CH str
	ν_{8a}	1800	1643	1627	1580	1580	$43S_1 + 11S_5$	CN, CC str; ring def
	ν_{19a}	1573	1458	1448	1390	1390	$18S_1 + 34S_4$	CC, CN str; ring def
	ν_{9a}	1260	1175	1168	1139	1139	$11S_2 + 15S_5 + 37S_9$	CH bend; CN, CC str, ring deformation
	ν_{12}	1165	1090	1085	1080	1080	$13S_1 + 20S_3 + 17S_9$	CN, CC str, CH bend; ring def
	ν_1	1102	1014	1012	972	972	$24S_3 + 40S_5$	CN, CC str
	ν_{6a}	751	693	697	665	665	$51S_2 + 30S_3$	ring def
B_1	ν_{7b}	3376	3228	3176	3086	3086	$98S_{10}$	CH stretching
	ν_{8b}	1801	1635	1625	1565	1565	$47S_{11} + 10S_{17}$	CH bend, CN,CC str; ring def
	ν_{19b}	1641	1518	1510	1470	1470	$17S_{11} + 46S_{12} + 12S_{13}$	CH bend
	ν_{14}	1519	1420	1409	1376	1376	$15S_{12} + 35S_{13} + 12S_{14}$	CH bend; CN,CC str; ring def
	ν_3	1360	1342	1270	1225	1225	$12S_{13} + 28S_{14} + 11S_{17}$	CH bend; CN,CC str; ring def
	ν_{15}	1213	1264	1235	1131	1136	$76S_{15}$	CC, CN str
	ν_{18b}	1164	1113	1101	1021	1021	$44S_{14} + 21S_{17}$	CN, CC str; ring def
	ν_{6b}	683	629	633	628	628	$31S_{16} + 18S_{17}$	CC, CN str; ring def
A_2	ν_{17a}	1131	976	1001	1020	1020	$92S_{19}$	torsion,wagging
	ν_{16a}	461	406	410	392	392	$91S_{18}$	torsion
B_2	ν_5	1156	989	1020	1070	1070	$10S_{22} + 77S_{24}$	torsion, wagging
	ν_{11}	1095	941	978	980	980	$11S_{21} + 12S_{22} + 50S_{23}$	wagging, torsion
	ν_{10b}	911	810	824	826	826	$46S_{22} + 24S_{23}$	wagging
	ν_4	788	733	738	722	722	$68S_{21}$	torsion
	ν_{16b}	416	449	354	344	344	$74S_{20} + 14S_{23}$	torsion, wagging

plane and out-of-plane normal modes. To compare the results of this work with those for other azines appearing in the literature[28,29] and given the similarity of results from different theoretical levels, we have chosen the MP2 calculation as a starting point for the refinement.

Although the most convenient structural parameters for this kind of analysis should be those from X-ray or neutron diffraction at low temperature,[38] we have chosen those from the MP2 calculation, because the X-ray structure does not reveal the hydrogen atom positions and no neutron diffraction data are available at present.

In all the cases, the strategy followed in the refinement was first to fit only the diagonal force constants until the difference between observed and calculated frequencies reached a minimum. The location of the important off-diagonal force constants was then determined, and these were then refined to obtain the best agreement between observed and calculated INS spectra. In our previous analysis of other azines,[28,29] only a very small number of off-diagonal terms were required to make a considerable improvement in the refinement. In the present work, however, all off-diagonal elements were required and the refinement of some of them proved decisive in reproducing the correct frequencies and intensities. The final force constants refined in symmetry coordinates are collected in Table 5 along with the initial values.

Our results for the in-plane A_1 and B_1 modes are in agreement with most of the previous assignments for pyrimidine. We confirm the assignments at 665 and 628 cm^{-1}, for the normal modes ν_{6a} and ν_{6b}, respectively, according to references 2 and 4−13 rather than those of Lord et al.[3] who assigned those at 624 and 567 cm^{-1}, respectively. In addition, we confirm the assignments for ν_{12} and ν_{18b} at 1080 and 1021 cm^{-1} in the polycrystalline sample. The small displacement from 1066 to 1080 cm^{-1} is probably due to the solid-state effects, Flogizzo and Novak[7] having observed ν_{12} at 1086 cm^{-1} in the crystal sample and at 1066 cm^{-1} in solution.

At present, INS spectroscopy is poorly adapted for measuring CH stretching normal modes due to the high Debye−Waller factor in this spectral region, this being imposed by instrumental constraints. We therefore attribute low statistical weight to this region in the force field analysis.

For the out-of-plane normal modes, the normal mode ν_{16a} is assigned at 392 cm^{-1}, this being very close to our MP2 and B3LYP calculations and also to the value calculated by Martin and Van Alsenoy,[19] using a different basis set in their B3LYP exchange correlation calculations. Our final assignment for ν_{17a} is at 1020 cm^{-1}, which is close to the value proposed by Wiberg[17] after scaling at 1016 cm^{-1}. We attempted to assign ν_{17a} at 980 cm^{-1} as proposed by Pongor et al.,[18] but this resulted in three intense INS features within a small frequency interval which is in conflict with the measured INS spectrum.

Considering the B_2 symmetry block, the normal mode ν_5 has been assigned to the band appearing at 1070 cm^{-1}, with the closest value calculated in the literature being that given by Wiberg[17] at 1041 cm^{-1}. This normal mode appears as an intense band in the INS spectrum, together with ν_{12}. Our assignment for ν_{11} at 980 cm^{-1} is in agreement with Martin and Van Alsenoy's predictions, who assigned it at 955 cm^{-1}. There is no INS feature near 955 cm^{-1}, but an intense band appears in the INS spectrum at 980 cm^{-1}. The other normal modes were readily assigned as isolated bands in the INS spectrum. Thus, ν_{10b} have been assigned to 826 cm^{-1}, close to 811 cm^{-1} as in previous reports. Again, the small shift is probably due to solid-state effects, Flogizzo et al.[7] having observed this band at 831 cm^{-1} in a single-crystal Raman experiment. We propose to assign ν_4 at 722 cm^{-1} corresponding to a intense band in the INS spectrum, which is in agreement with Foglizo et al.[7] and Bokobza-Sebagh et al.[12] Similarly, ν_{16b} appears at 344 cm^{-1} in agreement with all the previous vibrational analyses. We list observed and final calculated frequencies in Table 4.

It is interesting to note that the whole spectral intensity profile comes from the calculated atomic displacements which have to be distributed between internal mode peaks and their phonon wings. The distribution for the phonon wings is fitted with a single parameter, the Debye−Waller factor, which is the overall isotropic displacement of the molecule in its lattice modes. The final value for this parameter is 0.015, similar to those obtained in related azines.[28,29] Figure 3 shows the calculated INS spectrum

TABLE 5: Force Constants (aJ Å^{-2}) in Symmetry Coordinates for the Pyrimidine Molecule after the Refinement Procedure[a]

					A_1				
$F_{1,1}$	10.679 (8.573)								
$F_{2,2}$	0.0294 (−0.0233)	1.113 (0.667)							
$F_{3,3}$	−0.5418	−0.0251 (−0.0706)	1.681 (0.919)						
$F_{4,4}$	−0.1268	−0.1145	0.1379	6.106 (4.103)					
$F_{5,5}$	0.6964 (−0.2929)	0.1785	1.0699 (0.1680)	0.50266 (0.0266)	6.728 (8.119)				
$F_{6,6}$	0.0100	0.0950	0.0095	0.04630	−0.0361	5.038 (5.825)			
$F_{7,7}$	−0.2146	−0.0960	0.1330	0.0569	0.0141	0.0080	5.066 (5.715)		
$F_{8,8}$	−0.0210	−0.0148	0.0834	−0.1429	−0.1800	0.0007	−0.0024	5.176 (5.766)	
$F_{9,9}$	−0.7998 (−0.3045)	0.0101	0.0466	−0.0922	0.3425 (0.2121)	0.0065	−0.0282	0.0100	0.529 (0.635)
					B_1				
$F_{10,10}$	5.222 (5.712)								
$F_{11,11}$	0.0088	0.717 (0.668)							
$F_{12,12}$	0.0049	−0.0039	0.602 (0.520)						
$F_{13,13}$	0.0011	−0.0157	0.0092	0.592 (0.608)					
$F_{14,14}$	−0.0777	0.3669	0.1859	−0.1490	5.549 (7.617)				
$F_{15,15}$	−0.0850	0.2103	−0.0959	0.2499	0.0223 (−0.2457)	3.319 (4.701)			
$F_{16,16}$	0.0467	0.0290	0.0919	−0.0643	1.6417 (0.5493)	0.2571 (0.0570)	2.201 (0.880)		
$F_{17,17}$	0.1768	0.1458 (0.1545)	−0.0758	−0.1641	0.1125 (−0.1896)	0.4649 (−0.0508)	−1.3711 (−0.4439)	4.224 (4.774)	
					A_2				
$F_{18,18}$	0.216 (0.235)								
$F_{19,19}$	−0.0057 (−0.0042)	0.359 (0.325)							
					B_2				
$F_{20,20}$	0.202 (0.209)								
$F_{21,21}$	−0.0131	0.309 (0.339)							
$F_{22,22}$	−0.0027	−0.0125	0.283 (0.293)						
$F_{23,23}$	−0.0264 (−0.0324)	0.0308	0.0129 (0.0154)	0.304 (0.278)					
$F_{24,24}$	−0.0139	0.0164	−0.0294	0.0446	0.433 (0.333)				

[a] The initial values are in parentheses. The angle deformation coordinates have been scaled by 1 Å.

after the refinement together with the observed spectrum. As can be seen, the agreement between observed and calculated spectral intensities is good in almost the entire range studied, from which we infer that intermolecular interactions are relatively weak. The poor fit of the spectrum in the 1300−1600 cm^{-1} region is almost certainly due to a breakdown of the isotropic approximation.[39]

To assess the physical reality of our force field, we have carried out a comparison of the force constants matrix resulting from the INS refinement with those obtained by other authors. We have chosen the force field calculated by G. Pongor et al.[18] due to the fact that these authors collected the final force constants obtained for the pyrimidine molecule after the scaling procedure. Thus, we have transformed our force constants expressed in independent symmetry coordinates, those listed in Table 2, into the Pulay's coordinates system used in ref 18. To

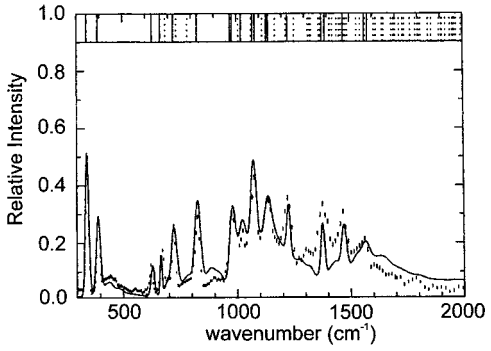

Figure 3. Observed (bars line) and calculated (continuous line) INS spectra of pyrimidine after refinement of symmetrized force constants. The conventions of this figure are the same as those for Figure 2.

TABLE 6: Comparison of the Force Constants Matrix in Pulay's Coordinates from This Work and that by G. Pongor et al. (ref 18)[a]

potential energy term	this work	ref 18	potential energy term	this work	ref 18	potential energy term	this work	ref 18
$\mathbf{R}_6\,\mathbf{R}_6$	6.367	6.567	$\beta_2\,\mathbf{r}_1$	0.0046	0.0027	$\mathbf{q}_{16}\,\mathbf{R}_4$	0.4610	−0.0427
$\mathbf{R}_5\,\mathbf{R}_6$	1.1804	0.8644	$\beta_2\,\mathbf{r}_4$	−0.0136	−0.0136	$\mathbf{q}_{16}\,\mathbf{R}_3$	0.4610	−0.0427
$\mathbf{R}_5\,\mathbf{R}_5$	7.561	7.045	$\beta_2\,\mathbf{r}_2$	−0.0146	−0.0136	$\mathbf{q}_{16}\,\mathbf{R}_2$	−0.4358	−0.3881
$\mathbf{R}_4\,\mathbf{R}_6$	−0.7832	−0.5062	$\beta_2\,\mathbf{r}_3$	0.0071	0.0053	$\mathbf{q}_{16}\,\mathbf{R}_1$	0.4163	0.2021
$\mathbf{R}_4\,\mathbf{R}_5$	0.9740	0.8064	$\beta_2\,\beta_2$	0.560	0.5459	$\mathbf{q}_{16}\,\mathbf{r}_1$	−0.0591	−0.0932
$\mathbf{R}_4\,\mathbf{R}_4$	7.203	7.121	$\beta_1\,\mathbf{R}_6$	−0.1559	−0.1489	$\mathbf{q}_{16}\,\mathbf{r}_4$	0.0307	0.0528
$\mathbf{R}_3\,\mathbf{R}_6$	−0.4470	0.5356	$\beta_1\,\mathbf{R}_5$	−0.0158	−0.0004	$\mathbf{q}_{16}\,\mathbf{r}_2$	0.0307	−0.0802
$\mathbf{R}_3\,\mathbf{R}_5$	−0.1648	−0.5033	$\beta_1\,\mathbf{R}_4$	0.0402	0.0328	$\mathbf{q}_{16}\,\mathbf{r}_3$	−0.0604	−0.0802
$\mathbf{R}_3\,\mathbf{R}_4$	1.8521	1.0970	$\beta_1\,\mathbf{R}_3$	−0.0402	−0.328	$\mathbf{q}_{16}\,\beta_2$	−0.0312	−0.0423
$\mathbf{R}_3\,\mathbf{R}_3$	7.206	7.121	$\beta_1\,\mathbf{R}_2$	0.0158	0.004	$\mathbf{q}_{16}\,\beta_1$	0.0000	0.0000
$\mathbf{R}_2\,\mathbf{R}_6$	0.0027	−0.4413	$\beta_1\,\mathbf{R}_1$	0.1559	0.1489	$\mathbf{q}_{16}\,\beta_4$	0.0312	0.0423
$\mathbf{R}_2\,\mathbf{R}_5$	2.6949	0.6840	$\beta_1\,\mathbf{r}_1$	0.0000	0.000	$\mathbf{q}_{16}\,\beta_3$	0.0000	0.0000
$\mathbf{R}_2\,\mathbf{R}_4$	−0.1648	−0.5033	$\beta_1\,\mathbf{r}_4$	0.0035	0.0003	$\mathbf{q}_{16}\,\mathbf{q}_{15}$	−0.2747	−0.0002
$\mathbf{R}_2\,\mathbf{R}_3$	0.9740	0.8064	$\beta_1\,\mathbf{r}_2$	−0.0035	−0.0003	$\mathbf{q}_{16}\,\mathbf{q}_{16}$	1.477	1.481
$\mathbf{R}_2\,\mathbf{R}_2$	7.561	7.045	$\beta_1\,\mathbf{r}_3$	0.0000	0.0000	$\mathbf{q}_{17}\,\mathbf{R}_6$	1.1473	0.1794
$\mathbf{R}_1\,\mathbf{R}_6$	1.3347	0.7007	$\beta_1\,\beta_2$	0.0065	0.0074	$\mathbf{q}_{17}\,\mathbf{R}_5$	1.0804	−0.1856
$\mathbf{R}_1\,\mathbf{R}_5$	0.0027	−0.4413	$\beta_1\,\beta_1$	0.602	0.4798	$\mathbf{q}_{17}\,\mathbf{R}_4$	−0.5498	−0.4114
$\mathbf{R}_1\,\mathbf{R}_4$	−0.4470	0.5356	$\beta_4\,\mathbf{R}_6$	0.1857	0.1447	$\mathbf{q}_{17}\,\mathbf{R}_3$	0.5498	0.4114
$\mathbf{R}_1\,\mathbf{R}_3$	−0.7832	−0.5062	$\beta_4\,\mathbf{R}_5$	−0.5798	−0.3004	$\mathbf{q}_{17}\,\mathbf{R}_2$	−1.0804	0.1856
$\mathbf{R}_1\,\mathbf{R}_2$	1.1804	0.8644	$\beta_4\,\mathbf{R}_4$	−0.0041	−0.0206	$\mathbf{q}_{17}\,\mathbf{R}_1$	−1.1473	−0.1704
$\mathbf{R}_1\,\mathbf{R}_1$	6.367	6.567	$\beta_4\,\mathbf{R}_3$	0.0505	0.0206	$\mathbf{q}_{17}\,\mathbf{r}_1$	0.0000	0.0000
$\mathbf{r}_1\,\mathbf{R}_6$	0.0448	0.0560	$\beta_4\,\mathbf{R}_2$	−0.2717	0.0040	$\mathbf{q}_{17}\,\mathbf{r}_4$	−0.0330	−0.0592
$\mathbf{r}_1\,\mathbf{R}_5$	−0.0119	−0.0141	$\beta_4\,\mathbf{R}_1$	0.0195	0.0123	$\mathbf{q}_{17}\,\mathbf{r}_2$	0.0330	0.0592
$\mathbf{r}_1\,\mathbf{R}_4$	−0.0110	−0.0239	$\beta_4\,\mathbf{r}_1$	−0.0046	−0.0027	$\mathbf{q}_{17}\,\mathbf{r}_3$	0.0000	0.0000
$\mathbf{r}_1\,\mathbf{R}_3$	−0.0110	−0.0239	$\beta_4\,\mathbf{r}_4$	0.0146	0.0136	$\mathbf{q}_{17}\,\beta_2$	0.0455	−0.0620
$\mathbf{r}_1\,\mathbf{R}_2$	−0.0119	−0.0141	$\beta_4\,\mathbf{r}_2$	0.0136	0.0136	$\mathbf{q}_{17}\,\beta_1$	−0.0919	0.0888
$\mathbf{r}_1\,\mathbf{R}_1$	0.0448	0.0560	$\beta_4\,\mathbf{r}_3$	−0.0071	−0.0053	$\mathbf{q}_{17}\,\beta_4$	0.0455	−0.0620
$\mathbf{r}_1\,\mathbf{R}_1$	5.038	5.286	$\beta_4\,\beta_2$	0.0318	−0.0107	$\mathbf{q}_{17}\,\beta_3$	−0.0290	0.049
$\mathbf{r}_4\,\mathbf{R}_6$	0.0809	−0.0076	$\beta_4\,\beta_1$	0.0065	0.0074	$\mathbf{q}_{17}\,\mathbf{q}_{15}$	0.0000	0.0000
$\mathbf{r}_4\,\mathbf{R}_5$	0.2206	−0.0245	$\beta_4\,\beta_4$	0.560	0.5459	$\mathbf{q}_{17}\,\mathbf{q}_{16}$	0.0000	0.00000
$\mathbf{r}_4\,\mathbf{R}_4$	−0.0274	−0.0127	$\beta_3\,\mathbf{R}_6$	−0.0191	−0.0032	$\mathbf{q}_{17}\,\mathbf{q}_{17}$	2.202	1.271
$\mathbf{r}_4\,\mathbf{R}_3$	−0.0024	−0.0243	$\beta_3\,\mathbf{R}_5$	0.0206	0.0241	$\gamma_1\,\gamma_1$	0.359	0.431
$\mathbf{r}_4\,\mathbf{R}_2$	−0.0072	0.1835	$\beta_3\,\mathbf{R}_4$	0.3237	0.2984	$\gamma_4\,\gamma_1$	0.0663	−0.0563
$\mathbf{r}_4\,\mathbf{R}_1$	−0.0098	0.0690	$\beta_3\,\mathbf{R}_3$	−0.3237	−0.2984	$\gamma_4\,\gamma_4$	0.399	0.4625
$\mathbf{r}_4\,\mathbf{R}_1$	0.0057	0.0134	$\beta_3\,\mathbf{R}_2$	−0.0206	−0.0241	$\gamma_2\,\gamma_1$	0.0663	−0.0563
$\mathbf{r}_4\,\mathbf{R}_4$	5.144	5.217	$\beta_3\,\mathbf{R}_1$	0.0191	0.0032	$\gamma_2\,\gamma_4$	−0.0174	−0.0201
$\mathbf{r}_2\,\mathbf{R}_6$	−0.0098	0.0690	$\beta_3\,\mathbf{r}_1$	0.0000	0.0000	$\gamma_2\,\gamma_2$	0.399	0.462
$\mathbf{r}_2\,\mathbf{R}_5$	−0.0072	0.1835	$\beta_3\,\mathbf{r}_4$	0.0062	0.0051	$\gamma_3\,\gamma_1$	−0.0964	−0.0344
$\mathbf{r}_2\,\mathbf{R}_4$	−0.0024	−0.0243	$\beta_3\,\mathbf{r}_2$	−0.0062	−0.0051	$\gamma_3\,\gamma_4$	−0.0550	−0.0052
$\mathbf{r}_2\,\mathbf{R}_3$	−0.0274	−0.0127	$\beta_3\,\mathbf{r}_3$	0.0000	0.0000	$\gamma_3\,\gamma_2$	−0.0550	−0.0052
$\mathbf{r}_2\,\mathbf{R}_2$	0.2206	−0.0245	$\beta_3\,\beta_2$	−0.0110	−0.0092	$\gamma_3\,\gamma_3$	0.389	0.462
$\mathbf{r}_2\,\mathbf{R}_1$	0.0809	−0.0076	$\beta_3\,\beta_1$	−0.0039	−0.0027	$\mathbf{q}_{22}\,\gamma_1$	−0.0035	0.1448
$\mathbf{r}_2\,\mathbf{R}1$	0.0057	0.0134	$\beta_3\,\beta_4$	−0.0110	−0.0092	$\mathbf{q}_{22}\,\gamma_4$	0.0242	−0.1162
$\mathbf{r}_2\,\mathbf{R}_4$	−0.0781	0.0022	$\beta_3\,\beta_3$	0.717	0.5774	$\mathbf{q}_{22}\,\gamma_2$	0.0242	−0.1162
$\mathbf{r}_2\,\mathbf{R}_2$	5.144	5.217	$\mathbf{q}_{15}\,\mathbf{R}_6$	−0.0839	0.0027	$\mathbf{q}_{22}\,\gamma_3$	−0.0134	−0.1245
$\mathbf{r}_3\,\mathbf{R}_6$	−0.0029	−0.0233	$\mathbf{q}_{15}\,\mathbf{R}_5$	0.2945	0.2423	$\mathbf{q}_{22}\,\mathbf{q}_{22}$	0.307	0.300
$\mathbf{r}_3\,\mathbf{R}_5$	−0.0118	−0.0203	$\mathbf{q}_{15}\,\mathbf{R}_4$	−0.2991	0.2297	$\mathbf{q}_{23}\,\gamma_1$	0.0007	0.1251
$\mathbf{r}_3\,\mathbf{R}_4$	0.1822	0.1532	$\mathbf{q}_{15}\,\mathbf{R}_3$	−0.2991	0.2297	$\mathbf{q}_{23}\,\gamma_4$	0.0219	−0.054
$\mathbf{r}_3\,\mathbf{R}_3$	0.1822	0.1532	$\mathbf{q}_{15}\,\mathbf{R}_2$	0.2945	0.2423	$\mathbf{q}_{23}\,\gamma_2$	0.0219	−0.054
$\mathbf{r}_3\,\mathbf{R}_2$	−0.0118	−0.0203	$\mathbf{q}_{15}\,\mathbf{R}_1$	−0.0839	0.0027	$\mathbf{q}_{23}\,\gamma_3$	0.0018	0.1079
$\mathbf{r}_3\,\mathbf{R}_1$	−0.0029	−0.0233	$\mathbf{q}_{15}\,\mathbf{r}1$	−0.0692	−0.0998	$\mathbf{q}_{23}\,\mathbf{q}22$	0.0020	0.0276
$\mathbf{r}_3\,\mathbf{R}1$	0.0007	0.0017	$\mathbf{q}_{15}\,\mathbf{r}_4$	0.0613	0.0748	$\mathbf{q}_{23}\,\mathbf{q}_{23}$	0.205	0.235
$\mathbf{r}_3\,\mathbf{R}_4$	0.0017	0.0039	$\mathbf{q}_{15}\,\mathbf{r}_2$	0.0613	0.0748	$\mathbf{q}_{24}\,\gamma_1$	0.0000	0.0000
$\mathbf{r}_3\,\mathbf{R}_2$	0.0017	0.0039	$\mathbf{q}_{15}\,\mathbf{r}_3$	0.0595	0.0713	$\mathbf{q}_{24}\,\gamma_4$	0.0057	0.1119
$\mathbf{r}_3\,\mathbf{R}_3$	5.176	5.305	$\mathbf{q}_{15}\,\beta_2$	0.0128	0.0111	$\mathbf{q}_{24}\,\gamma_2$	−0.0057	−0.1119
$\beta_2\,\mathbf{R}_6$	−0.0195	−0.0123	$\mathbf{q}_{15}\,\beta_1$	0.0000	0.0000	$\mathbf{q}_{24}\,\gamma_3$	0.0000	0.0000
$\beta_2\,\mathbf{R}_5$	0.2717	−0.0040	$\mathbf{q}_{15}\,\beta_4$	−0.0128	−0.0111	$\mathbf{q}_{24}\,\mathbf{q}_{22}$	0.0000	0.0000
$\beta_2\,\mathbf{R}_4$	−0.0505	−0.0216	$\mathbf{q}_{15}\,\beta_3$	0.0000	0.0000	$\mathbf{q}_{24}\,\mathbf{q}_{23}$	0.0000	0.0000
$\beta_2\,\mathbf{R}_3$	0.0041	0.0206	$\mathbf{q}_{15}\,\mathbf{q}_{15}$	1.319	1.337	$\mathbf{q}_{24}\,\mathbf{q}_{24}$	0.216	0.232
$\beta_2\,\mathbf{R}_2$	0.5798	0.3004	$\mathbf{q}_{16}\,\mathbf{R}_6$	0.4163	0.201			
$\beta_2\,\mathbf{R}_1$	−0.1857	−0.1447	$\mathbf{q}_{16}\,\mathbf{R}_5$	−0.4358	−0.3881			

[a] Units are consistent with energy measured in aJ, stretching and bending coordinates in Å and radian, respectively. Internal coordinates are defined according to ref 18.

achieve this, we have used the expression proposed by E. Martínez et al.[40] which let us to transform the force constants matrix, $\mathbf{F}_j$, referred to the *j*-system of independent coordinates, into another *i*-system of independent coordinates, $\mathbf{F}_i$, as follow:

$$\mathbf{F}_i = (\mathbf{B}_i\mathbf{B}^t_i)^{-1}\,\mathbf{B}_i\mathbf{B}^t_j\mathbf{F}_j\mathbf{B}_j\mathbf{B}^t_i\,(\mathbf{B}_i\mathbf{B}^t_i)^{-1} \qquad (1)$$

where $\mathbf{B}_i = \mathbf{U}_i\mathbf{b}_i$, $\mathbf{U}_i$ being the orthogonal matrix relating the independent symmetry coordinates to the dependent internal ones, $\mathbf{b}_i$ is the matrix relating the internal coordinates to the Cartesian coordinates, and $\mathbf{B}^t$ is the transpose of the $\mathbf{B}$ matrix. The force constants obtained after the transformation are listed in Table 6. As can be seen, the *diagonal* force constants resulting

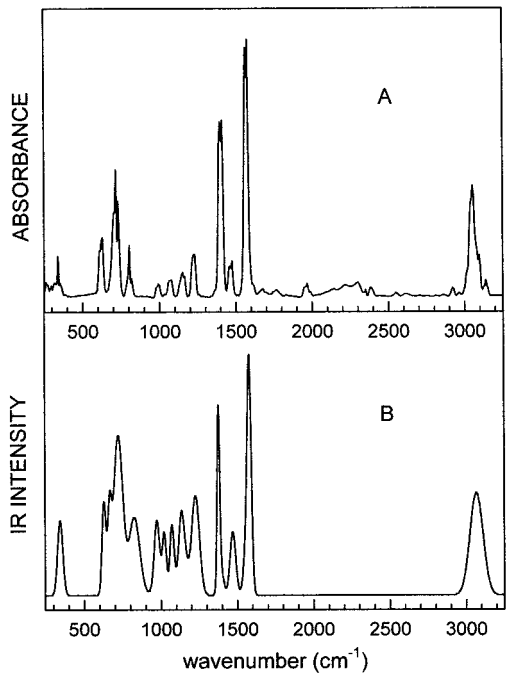

Figure 4. Observed (A) and calculated (B) IR spectra of the pyrimidine molecule.

from the INS refinement are similar to those obtained by G. Pongor et al.[18] except in the case of the coordinate $q_{17,}$ which corresponds to a linear combination of ring deformation, taking the value of 2.202 mdyn/Å in this work and 1.271 mdyn/Å in ref 18. On the other hand, larger differences are obtained for the *off-diagonal* force constants. This fact is not surprising because the INS intensity is very sensitive to off-diagonal force constants, and as can be seen in Table 5, some of them have been modified from the initial value, even in sign, during the refinement procedure in order to reproduce not only the wavenumber but also the intensity.

Finally, we have calculated the IR spectrum from the present force field. For this we have used the CLIMAX program which let us calculate the IR intensity for a normal mode, ν, through the atomic displacements matrix and q_i, the atomic charge calculated at the MP2/6-31G* level.[26] The calculated IR intensity has been simulated by a Gaussian profile. To our knowledge, there are not any gas-phase integrated intensities for the pyrimidine molecule, and therefore, we can only perform a qualitative comparison between the observed and calculated infrared spectra. In Figure 4, we show the calculated IR spectrum along with the corresponding observed one in the gas phase. As can be seen, there exists good correspondence between the observed and calculated spectrum, except for the modes in the 1300−1500 cm^{-1}, where the calculated intensity is lower than the observed one. This is in accord with the poorer fit for this region in the INS spectrum which could originate the same defect for these modes in the IR spectrum.

V. Conclusions

We have carried out a rigorous vibrational analysis for all the normal modes of the pyrimidine molecule using INS combined with quantum mechanical calculations. For this, we have accomplished geometry optimization and frequencies calculations at three different levels of theory in the Hamiltonian operator, using the same basis set. Our results point out that the correlation effects must be taken into account in order to reproduce geometry as well as wavenumbers for pyrimidine.

However, despite the very good agreement between observed and calculated frequencies from MP2 and B3LYP calculations, the calculated INS intensity does not reproduce the observed INS spectrum well. Therefore, a normal coordinates analysis in symmetry coordinates has been carried out for pyrimidine, refining the force constants matrix in order to obtain the better atomic displacements of this molecule in the solid state. A good agreement between the observed and calculated spectra shows that the isolated-molecule approximation can be used in this case. This has allowed us to provide a more confident set of assignments than was possible previously.

The force field resulting from the INS refinement has been validated by comparing it with that obtained by G. Pongor et al.,[18] obtaining similar results for the diagonal force constants. In addition, the IR spectrum has been calculated from the atomic displacement matrix calculated from our force field with satisfactory results.

Acknowledgment. We are grateful to ISIS for enabling us to record the INS spectrum and the European Community for providing financial support.

References and Notes

(1) Porter, A. E. A. In *Comprehensive Organic Chemistry*; Barton, D. D., Ollis, W. D., Sammes, P. G., Eds.; Pergamon Press: London, 1979; Vol. 4.
(2) Ito, M.; Shimada, R.; Kuraishi, T.; Mizushima, W. *J. Chem. Phys.* **1956**, *25*, 597.
(3) Lord, R. C.; Marston, A. J.; Miller, F. A. *Spectrochim. Acta* **1957**, *9*, 113.
(4) Innes, K. K.; Merritt, J. A.; Tincher, W. C.; Tilford, S. G. *Nature* **1969**, *187*, 500.
(5) Simmons, J. D.; Innes, K. K. *J. Mol. Spectrosc.* **1964**, *13*, 435.
(6) Sbrana, G.; Adembri, G.; Califano, S. *Spectrochim. Acta* **1966**, *22*, 1831.
(7) Foglizzo, R.; Novak, A. *J. Chim. Phys.* **1967**, *64*, 1484.
(8) Innes, K. K.; Byrne, J. P.; Ross, I. G. *J. Mol. Spectrosc.* **1967**, *22*, 125.
(9) Foglizzo, R. *Spectrosc. Lett.* **1969**, *2*, 165.
(10) Innes, K. K.; McSwiney, H. D., Jr.; Simmons, J. D.; Tilford, S. G. *J. Mol. Spectrosc.* **1969**, *31*, 31.
(11) Milani-Nejad, F.; Stidham, H. D. *Spectrochim. Acta* **1975**, *31A*, 1433.
(12) Bokobza-Sebagh, L.; Zarembowitch, J. *Spectrochim. Acta* **1976**, *32A*, 797.
(13) Unemoto, M.; Ogata, T.; Shimada, H.; Shimada, R. *Bull. Chem. Soc. Jpn.* **1984**, *57*, 3300.
(14) Berezin, V. I.; Potapov, S. K. *Opt. Spectroc.* **1965**, *18*, 22.
(15) Anantharama Sharma, Y. *Spectrochim. Acta* **1974**, *30A*, 1801.
(16) Magdo, I.; Pongor, G.; Fogarasi, G. *J. Mol. Struct. (THEOCHEM)* **1994**, *303*, 243.
(17) Wiberg, K. B. *J. Mol. Struct.* **1990**, *244*, 61.
(18) Pongor, G.; Fogarasi, G.; Magdó, I.; Boggs, J.; Keresztury, J.; Innatyev, I. S. *Spectrochim. Acta* **1992**, *48A*, 111.
(19) Martin, J. M. L.; Van Alsenoy, C. *J. Chem. Phys.* **1996**, *100*, 6973.
(20) Amouche, A.; Ghomi, M.; Columbeau, C.; Jobic, H.; Grajcar, L.; Baron, M. H.; Turpin, P. Y.; Henriet, C.; Berthier, G. *J. Phys. Chem.* **1996**, *100*, 5224.
(21) Amouche, A.; Berthier, G.; Columbeau, C.; Flament, J. P.; Ghomi, M.; Henriet, C., Jobic, H.; Turpin, P. Y. *Phys. Chem.* **1996**, *204*, 253.
(22) Kearley, G. J. *Spectrochim. Acta* **1992**, *48A*, 349.
(23) Tomkinson, J. *Spectrochim. Acta* **1991**, *48A*, 329.
(24) Tomkinson, J. In *Recent Experimental and Computational Advances in Molecular Spectroscopy*; Fausto, R., Ed.; Kluwer Academic Publishers: The Netherlands, 1993.
(25) Bée, M. In *Quasielastic Neutron Scattering*; Adam Hilger: Bristol, 1988.
(26) Wilson, E. B., Jr.; Decius, J. C.; Cross, P. C. In *Molecular Vibrations*; McGraw-Hill: New York, 1955.
(27) Kearley, G. J. *J. Chem. Soc., Faraday Trans. 2* **1986**, *82*, 41.
(28) Navarro, A.; López Gonzalez, J. J.; Kearley, G. J.; Tomkinson, J.; Parker, S. F.; Sivia, D. S. *Chem. Phys.* **1995**, *200*, 395.
(29) Kearley, G. J.; Tomkinson, J.; Navarro, A.; López González, J. J.; Fernández Gómez, M. *Chem. Phys.* **1997**, *216*, 323.
(30) Frish, M.; Trucks, G. W.; Schlegel, H. B.; Gill, P. M. W.; Johnson, B. G.; Robb, M. A.; Cheeseman, J. R.; Keith, T.; Peterson, G. A.;

Montgomery, J. A.; Raghavachari, K.; Al-Laham, M. A.; Zakrzewski, V. G.; Ortiz, J. V.; Foresman, J. B.; Cioslowski, J.; Stefanov, B. B.; Nanayakkara, A.; Challacombe, M.; Peng, C. Y.; Ayala, P. Y.; Chen, W.; Wong, M. W.; Andres, J. L.; Replogle, E. S.; Gomperts, R.; Martin, R. L.; Fox, D. J.; Binkley, J. S.; Defrees, D. J.; Baker, J.; Stewart, J. P.; Head-Gordon, M.; Gonzalez, C.; Pople, J. A. *GAUSSIAN 94*, revision B.1; Gaussian, Inc.: Pittsburgh, 1995.

(31) Hehre, W. J.; Radom, L.; Scheleyer, P. V. R.; Pople, J. A. *Ab initio Molecular Orbital Theory*; Wiley: New York, 1986.

(32) Möller, C.; Plesset, M. S. *Phys. Rev.* **1934**, *46*, 618.

(33) (a) Lee, C.; Yang, W.; Parr, R. G. *Phys. Rev.* **1988**, *B37*, 785. (b) Becke, A. D. J. *Chem. Phys.* **1993**, *98*, 5648.

(34) Zerbi, G. In *Vibrational Spectroscopy-Modern Trends*; Barnes, A. J., Orville-Thomas, M. J., Eds.; Elsevier: Amsterdam, 1977.

(35) Tomkinson, J.; Warner, M.; Taylor, A. D. *Mol. Phys.* **1984**, *51*, 381.

(36) Howard, J.; Boland, C. B.; Tomkinson, J. *Chem. Phys.* **1983**, *777*, 145.

(37) Fernholt, L.; Romming, C. *Acta Chem. Scand.* **1978**, *32A*, 271.

(38) Jeffrey, G. A. In *Accurate Molecular Structures. Their determination and importance*; Domenicano, A., Hargittai, J., Eds.; Oxford University Press: New York, 1992.

(39) Tomkinson, J.; Kearley, G. J. *Nucl. Instrum. Methods Phys. Res. A* **1995**, *354*, 169.

(40) Martínez Torres, E.; López González, J. J.; Fernández Gómez, M. *J. Chem. Phys*. **1999**, *110*, 3302.